Stimulus-dependent refractoriness in the Frankenhaeuser-Huxley model

R.P. Morse*, D. Allingham[1], N. G. Stocks

School of Engineering, University of Warwick, Coventry, CV4 7AL, UK

[1] Present address:

D. Allingham
School of Mathematical and Physical Sciences
University of Newcastle
Callaghan, NSW, 2308
Australia

E-mail Addresses:

R.Morse@warwick.ac.uk (R.P. Morse)
David.Allingham@newcastle.edu.au (D. Allingham)
N.G.Stocks@warwick.ac.uk (N.G. Stocks)

**Corresponding author:*

Tel: +44(0)24 765 22857
Fax +44(0)24 76 418922

Abstract

Phenomenological neural models, such as the leaky integrate-and-fire model, normally have a fixed refractory time-course that is independent of the stimulus. The recovery of threshold following an action potential is typically based on physiological experiments that use a two-pulse paradigm in which the first pulse is suprathreshold and causes excitation and the second pulse is used to determine the threshold at various intervals following the first. In such experiments, the nerve is completely unstimulated between the two pulses. This contrasts the receptor stimuli in normal physiological systems and the electrical stimuli used by cochlear implants and other neural prostheses. A numerical study of the Frankenhaeuser-Huxley conductance-based model of nerve fibre was therefore undertaken to investigate the effect of stimulation on refractoriness. We found that the application of a depolarizing stimulus during the later part of what is classically regarded as the absolute refractory period could effectively prolong the absolute refractory period, while leaving the refractory time-constants and other refractory parameters largely unaffected. Indeed, long depolarizing pulses, which would have been suprathreshold if presented to a resting nerve fibre, appeared to block excitation indefinitely. Stimulation during what is classically regarded as the absolute refractory period can therefore greatly affect the temporal response of a nerve. We conclude that the classical definition of absolute refractory period should be refined to include only the initial period following an action potential when an ongoing stimulus would not affect threshold; this period was found to be about half as long as the classical absolute refractory period. We further conclude that the stimulus-dependent nature of the relative refractory period must be considered when developing a phenomenological nerve model for complex stimuli.

Keywords: Frankenhaeuser-Huxley, nerve model, refractory period, cochlear implant.

1. Introduction

All nerve fibres, whether sensory or motor, exhibit certain common features, including a threshold "all-or-nothing" response and refractoriness, the phenomenon where the threshold following an action potential (nerve spike) is temporarily higher than the resting threshold. The refractory period is conventionally divided into two parts: the "absolutely refractory period" (Gotch, 1910; Gotch and Burch, 1899), during which the fibre is unable to generate another spike regardless of the stimulus, followed immediately by the "relative refractory period", during which sufficiently large depolarization of the nerve fibre can evoke an action potential (Adrian and Lucas, 1912; Adrian, 1914; Gotch, 1910). During the absolute refractory period a nerve fibre's threshold is deemed infinite and during the relative refractory period the threshold relaxes towards its resting value. Such refractoriness greatly affects the temporal response of a nerve fibre to a stimulus.

In many neural models that are intended to be predictive and used, for example, to investigate the response of a nerve fibre to electrical stimulation by a cochlear implant (e.g. Bruce et al., 1999; White, 1985; Xu and Collins, 2004) or for more fundamental physiological studies of neural coding (e.g. Borst et al., 2004; Bugmann, 1997; Chapeau-Blondeau et al., 1996), the refractory time-course follows a fixed time-course independent of the stimulus. We have previously (Morse and Evans, 2003), however, recorded the single fibre response of the sciatic nerve of the toad *Xenopus laevis* to a very wide range of stimulus levels and frequencies (levels up to 24 dB above threshold, frequencies from 50 Hz to 2 kHz). An inspection of the discharge rate-level functions for a single fibre over a range of stimulus

frequencies suggested that the data could not be modelled by a fixed refractory time course (Morse et al., 2014): for example, the maximum discharge rate in response to a 100-Hz signal was 100 spikes / s for all fibres, whilst the maximum discharge rate in response to a 2-kHz stimulus could be as high as 2000 spikes / s; this result shows that the absolute refractory period in response to the 2 kHz stimulus must be less than 0.5 ms, but if such a value is used in a leaky integrate-and-fire model with a fixed refractory time-course then with a high stimulus level it can lead to multiple discharges in response to each excitatory phase of a 100-Hz stimulus. This contrasts the physiological data, in which each excitatory phase of a low-frequency stimulus typically leads to one discharge. The prediction for the low-frequency rate-level functions could be improved by using a larger refractory period, but this led to a gross underestimation of the discharges evoked in response to high-frequency stimulation. A contrast between physiological data and results from a simple computational model was also found by Litvak et al. (2003); their computational model using physiologically-obtained refractory time-constants for cat cochlear nerve greatly over-predicted the maximum number of action potentials in response to a 5-kHz pulse train. As described below, we considered that predictive phenomenological models might be improved if the refractory time-course was stimulus dependent.

Many previous physiological studies have examined the refractoriness of particular nerves using a two-pulse paradigm, where the first pulse is suprathreshold and the threshold amplitude of the second pulse is measured for various intervals following the first pulse (e.g. Amberson, 1930; Erlanger et al., 1927; Forbes et al., 1923; Miller et al., 2001); the first pulse can be considered a conditioning pulse and the second a probe pulse. In this paradigm, the nerve is unstimulated between the discharges evoked by the conditioning and probe pulses.

This markedly contrasts our experiments with sinusoidal stimulation (Morse and Evans, 2003) and cochlear-implant experiments investigating the response to high-rate conditioners (e.g. Litvak et al., 2003), for which the stimulation is continuous; such continuous stimulation could affect recovery from refractoriness in a stimulus-dependent manner.

The purpose of this study was to determine whether stimulation during the refractory period affects threshold recovery following an action potential. In this study, we have extended the standard two-pulse paradigm to a three-pulse paradigm where the intermediate pulse occurs while the nerve is refractory. A three-pulse paradigm has previously been used by Rosenblueth et al. (1949) in a study of the refractory properties of cat nerve. In this study, however, interpretation of the results was hindered by the measurement of compound action potentials, the ensemble response of many fibres, rather than single-fibre responses. Moreover, the properties of the intermediate pulse were not varied systematically. We have undertaken a computational study of refractoriness using the Frankenhaeuser-Huxley model, which is a model of ion-channel permeability based on physiological data from the sciatic nerve of *Xenopus laevis* (Frankenhaeuser and Huxley, 1964); the model therefore directly corresponds to the nerve we have used in our physiological studies (Morse and Evans, 2003). Use of the computational model enabled an investigation into the effect of short-duration probe and conditioner pulses without the stimulus artefact problems that are associated with high-level stimulation of a physiological preparation (Miller et al., 2000). Here, we systematically varied the amplitude and duration of the intermediate pulse and show that the characteristics of the intermediate pulse do affect threshold recovery.

2. The Frankenhaeuser-Huxley nerve model

The Frankenhaeuser-Huxley (FH) model (1964) models the response of a sciatic nerve fibre of the toad *Xenopus laevis* at a single node of Ranvier. The model contains five differential equations and thirty-six parameters, and describes the course of a fibre's membrane potential following or during electrical stimulation. For reference, the model is briefly described in Appendix A using the nomenclature of the original paper. A key component of the model is the simulation of the activation and inactivation states of the sodium channels (represented by *m* and *h*, respectively), the activation state of the potassium channel (represented by *n*) and the activation state of a nonspecific ion channel (represented by *p*). The modern understanding is that these activation and inactivation variables represent the gating kinetics of the various ion channels. They are each determined by a one-dimensional ordinary differential equation that is both time- and voltage-dependent. Calculation of these variables enables the various ionic currents and the capacitative current to be calculated, and this enables the membrane voltage to be determined.

Numerical integration was done using the Heun method with a fixed time-step of 5 μs. We used parameter values, constants and initial conditions as reported by Frankenhaeuser and Huxley for their model at 20 °C (Frankenhaeuser and Huxley, 1964); because the simulations were at 20 °C, the standard temperature for the model, no correction for temperature was required (Frankenhaeuser and Moore, 1963; Rattay, 1990). The first 1 ms of each simulation was taken to be transient and after this time the model variables were all in a steady-state without stimulation. The conditioning pulse was presented only after this transient period had elapsed.

Because the FH model simulates the toad sciatic nerve at only a single node of Ranvier, some criterion was required to determine whether a spike was large enough to successfully

propagate along the nerve. In accord with data recorded from the vagus and saphenous nerve of cat (Paintal, 1966), and consistent with models by Frijns and ten Kate (1994), we deemed that a spike would propagate if its amplitude was 40 mV above the resting potential, which is about 34 % of the amplitude of the spike invoked by the conditioning pulse. For large stimuli in the refractory period, the contribution to the membrane voltage from the capacitive current, which is non-regenerative, can still cause this threshold to be exceeded. To prevent false spike detection, we multiplied the membrane voltage by a blanking signal that was zero from 25 μs before each conditioning and probe pulse to 150 μs after, and unity otherwise (Fig. 1). Fluctuations in membrane voltage that were outside the blanking periods and above 40 mV were considered to be real spikes that would propagate along the whole length of the nerve. Qualitatively identical results to those reported below were obtained using an alternative criterion of 60 %.

3. Numerical experiments

3.1. Two-pulse paradigm: baseline results

To obtain baseline results, we first replicated the two-pulse paradigm used in physiological studies. The conditioning pulse had a duration of 10 μs and an amplitude 1 dB[2] above the resting threshold of 60.61 A / m^2, which was found using the PEST algorithm (Taylor and Creelman, 1967; Wald level 0.5, target probability 0.5). The amplitude of the conditioner was sufficient to ensure excitation in response to every presentation and the short pulse duration of 10 μs was chosen to approximate a near-instantaneous application of current. A common way to determine the recovery function is to vary the time between the conditioner

[2] Absolute level = reference level x $10^{(\text{dB level} / 20)}$

and probe pulse and find the probe threshold for each interval pulse (e.g. Amberson, 1930; Erlanger et al., 1927; Forbes et al., 1923; Miller et al., 2001). However, because of the very rapid change in threshold immediately following the absolute refractory period, the changes in probe interval must be small if the spacing is constant. The simulations would therefore be time consuming. Alternatively, the spacing of the probe intervals could be small close to the absolute refractory period and spaced further apart at longer intervals. This is more efficient but requires knowledge of the duration of the absolute refractory period in advance. Throughout this study we have therefore determined threshold recovery by finding the minimum conditioner-probe interval that leads to excitation for various fixed probe amplitudes from threshold (0 dB) to 18 dB above the resting threshold for a 10-μs pulse. This method is insensitive to changes in the absolute refractory period and enables efficient measurement of threshold recovery.

The threshold recovery of the model following the conditioning pulse is shown in Fig. 2 and follows that expected from physiological experiments. For short intervals, less than about 1.3 ms, the threshold was effectively infinite and the model would conventionally be considered to be in an absolute refractory state. During the following 10 ms, the model was relatively refractory and the threshold gradually returned to its resting value (for clarity, Fig 2 shows only the 5 ms of the simulation). To characterize threshold recovery, the threshold during the relative refractory period has typically been fitted by an exponential function (e.g. Bruce et al., 1999), although other functions, e.g. hyperbolic (Buller et al., 1953), have been used (see Holden, 1976 for review). We have used a two time-constant exponential function (Morse and Evans, 2003) and the threshold during the relative refractory period, $\theta(t)$, was given by:

$$\theta(t) = \frac{\theta_{\text{rest}}}{1 - k\exp(\frac{\tau_{\text{abs}} - t}{\tau_1}) - (1-k)\exp(\frac{\tau_{\text{abs}} - t}{\tau_2})}, \quad (1)$$

where t is the time since the conditioning pulse was applied, $k \in [0, 1]$ is the relative weighting between the two time-constants, τ_{abs} is the duration of the absolute refractory period, and τ_1 and τ_2, represent the slow long-term and fast initial threshold recovery, respectively. We performed a comparison of Equation (1) with the equivalent single time-constant form, obtained by setting k to 1 in Equation (1), that is:

$$\theta(t) = \frac{\theta_{\text{rest}}}{1 - \exp(\frac{\tau_{\text{abs}} - t}{\tau_1})}. \quad (2)$$

Because both equations tend to infinity for small t, fits to simulation data using a least-squares approach to the recovery functions in their standard form, as in Equations 1 and 2, were not well behaved because very small random errors in the measured intervals could lead to very large squared-differences between the measurements and the fits; the fitted parameters, particularly the short time constant, τ_1, were therefore overly sensitive to random error. We therefore reparameterized the recovery functions and fitted the free parameters to $1 / \theta(t)$.

Fig. 2 shows the best fits to the single and double exponential models for threshold recovery. The two time-constant model (Equation 1) gave an excellent fit to the simulated threshold recovery (τ_{abs} = 1.23 ms, τ_1 = 1.65 ms, τ_2, = 0.25 ms, k = 0.46). The single time-constant function led to a reasonable fit of the simulated data for longer conditioner-probe intervals but did not give a good fit to shorter conditioner-probe intervals closer to the absolute refractory period. Because the two-time- constant recovery function gave a

substantially better fit, it was used to fit the threshold recovery data for the following study using a three-pulse paradigm.

3.2. Three-pulse paradigm

Following the baseline study, we investigated the effect of a depolarizing stimulus during the refractory period on refractory properties. This was done by introducing another pulse, between the suprathreshold conditioning pulse and the probe pulse used to determine threshold; the conditioning and probe pulses were 10 μs (identical to those in Section 3.1). The onset of the intermediate pulse immediately followed the conditioning pulse to represent continuous stimulation (see Fig. 3 for an example stimulus). For ease of reference, the amplitudes of the intermediate pulse are also given in dB relative to the resting threshold for a 10-μs pulse, and they ranged from 30 dB below threshold to 6 dB below threshold in 12-dB steps. The smallest duration of the intermediate pulse was 250 μs and we increased the duration in increments of 250 μs. If the end of the intermediate pulse exceeded the absolute refractory period then it would temporally summate with the probe pulse. As described below, however, the intermediate stimulus could effectively prolong the absolute refractory period and this effect was dependent on the amplitude of the intermediate pulse. The maximum duration of the intermediate pulse was therefore equal to the effective absolute refractory period for the particular amplitude of the intermediate pulse. For each duration and amplitude of the intermediate pulse, the threshold recovery function was determined and characterized using the methods in Section 3.1.

Threshold recovery functions for the three-pulse paradigm with an intermediate pulse duration of 1000 μs at various amplitudes are shown in Fig. 4. For each amplitude of the

intermediate pulse, the fitted curve was in excellent agreement with the simulated thresholds from the Frankenhaeuser-Huxley model. The most noticeable effect of the intermediate pulse was to prolong the absolute refractory period. Fig. 5 shows the fitted parameters for the double exponential recovery function (Equation 1) for the full range of intermediate pulse amplitudes and durations. The fitted curves were similar to those shown in Fig. 2 and Fig. 4 and remained in excellent agreement with the simulated values. For the range of intermediate pulse amplitudes studied, the effect of the intermediate pulse duration on the two time-constants of the recovery function (τ_1 and τ_2) and the weighting factor, k, was insubstantial (Figs. 5a to 5c). As introduced above, the main effect of the intermediate pulse was on the fitted value of the absolute refractory period (Fig. 5d). There was no effect on the measurement of τ_{abs} for intermediate pulses with a duration less than about 750 μs after the conditioning pulse. Once the intermediate pulse exceeded 750 μs, however, the measured absolute refractory period was extended by its presence. This effect was observed even when the intermediate pulse would have been subthreshold if presented to the resting nerve, e.g., for a 1000-μs pulse the threshold was 3.56 A / m^2 and a stimulus level of 1.92 A / m^2 (-30 dB relative to the 10-μs threshold) prolonged the absolute refractory period. As the amplitude of the intermediate pulse increased, the prolongation of the absolute refractory period became more pronounced and for pulses -6 dB relative to the 10-μs threshold the measured absolute refractory period appeared to extended indefinitely. In other words, the presentation of a depolarizing stimulus shortly after an action potential can suppress all future spikes regardless of the amplitude of subsequent stimulation; this suppression could occur even when the intermediate pulse could evoke a nerve spike when presented in isolation to the resting fibre. The effect of a depolarizing stimulus during the refractory period can therefore

be substantial.

The effect of the intermediate pulse on threshold recovery results directly from its temporal effect on the activation and inactivation variables of the Frankenhaeuser-Huxley model. As shown in Fig. 6 for various amplitudes of a 2000-μs intermediate pulse following a 10-μs conditioning pulse that was 1 dB above threshold, the intermediate pulse generally had a small effect on the phase spaces for the activation and inactivation variables: the only notable exception was that the maximum value of the potassium activation variable, *n*, increased for the largest amplitude of the intermediate pulse. In all cases there was still a characteristic trajectory back to the stable fixed point associated with the resting potential. The most pronounced effect of the intermediate pulse was to prolong the trajectory back to the stable point, that is to delay the return of the gating variables to their resting values. This is most clearly shown by the plots of the individual time courses of the activation and inactivation variables in Fig. 7. For the potassium activation variable, *n*, and the non-specific activation variable, *p*, an increase in the amplitude of the intermediate pulse led to a slightly faster rise time of each variable, a greater maximum level, and a markedly longer time to return to the resting value. The intermediate pulse had a negligible effect on the initial time course of the sodium inactivation variable, *h*, and, except for large values of the intermediate pulse, it had only a small effect on the minimum value of *h*; an increase, however, in the intermediate pulse amplitude also led to a markedly longer time for *h* to return to its resting value. Similarly, the intermediate pulse had a negligible effect on the rise time and most extreme value for the sodium activation variable, *m*; again, however, high levels of the intermediate pulse slowed the return of this gating variable to its resting value.

It follows directly from the results in the previous section that continued stimulation during the absolute refractory period following excitation by a sinusoidal stimulus would be expected to affect threshold recovery. This is demonstrated in Fig. 8 for a 100-Hz sinewave. Fig. 8a shows one period of a 100-Hz sinewave that was 12 dB above the resting threshold (3.52 A / m^2) preceded by a 1-ms gap. The cathodic (excitatory) phase of this stimulation, which is shown in Fig. 8a as positive values of the current density, led to a single action potential that exceeded the criterion threshold level of 40 mV (Fig. 8c). In contrast, if there was a sufficient gap in the stimulation during the absolute refractory period, for example between 2 and 3.5 ms as shown in Fig. 8b, then two action potentials could be evoked by the cathodic stimulation (Fig. 8d). Furthermore, the complementary stimulus, that is a stimulus that mirrors the stimulus gap (Fig. 8e), could cause excitation (Fig. 8f). In other words, a segment of a sinewave that in isolation causes excitation can lead to suppression of an action potential if it falls within the absolute refractory period.

4. Discussions and conclusions

We have shown that stimulation during the duration of the absolute refractory period, as measured using a two-pulse paradigm, can extend the duration of the measured absolute refractory period in the FH model. This supports the finding by Rosenblueth et al. (1949) that a short depolarizing pulse applied shortly before the probe pulse can block excitation in response to the probe.

Our findings are consequential for the terminology used for refractoriness and the classification of the refractory period into absolute and relative components. As pointed out by Forbes et al. (1923) and Rosenblueth et al. (1949), the classical classification of the

refractory period into absolute and relative components is not satisfactory because a stimulus applied during the interval in which another action potential cannot propagate, nominally the absolute refractory period, can cause excitation after the period has elapsed; the second action potential can result from the local response to the second stimulus, but can only be initiated after the "functional" absolute period has elapsed. Nonetheless, the terminology is widespread. Our finding that the measured absolute refractory period can be extended by a depolarizing stimulus appears to make the terminology worse. We therefore take the absolute refractory period to be the period during which an on-going stimulus would not affect the refractory parameters and is thus truly "absolute". In our simulations this was about 0.7 ms and about half the duration of the absolute refractory period measured with a classical two-pulse paradigm. We take the following period to be relatively refractory even though the nerve may have an infinite threshold during this period. We therefore consider the intermediate pulse in our study to affect only the relative refractoriness of the nerve.

We chose to study the effect of an intermediate pulse with the Frankenhaeuser-Huxley model because it is based on the same animal (the toad *Xenopus laevis*) we have used in physiological studies. The dynamics of this model, however, are broadly similar to those in the more well-known Hodgkin-Huxley model of the unmyelinated squid axon (Hodgkin and Huxley, 1952); the same effect of an intermediate pulse might therefore be expected with this model. There have been attempt to reduce the dimensionality of the Hodgkin-Huxley equations, most notably in the Fitz-Hugh Nagumo model (Fitzhugh, 1961; Nagumo et al., 1962) but also in studies by Abbott and Kepler (1990) and others. These models inherently model the dynamics of the activation and inactivation variables and may demonstrate a similar effect of an intermediate pulse on refractoriness. These models, however, are

intended to be analytically tractable rather than predictive. As introduced above, it is often necessary or desirable to use phenomenological models, such as the leaky integrate-and-fire model, to predict the response to electrical stimulation (see, e.g., Abbott and Kepler, 1990; Tuckwell, 1988). Due to their abstraction, however, most phenomenological models do not contain an implicit refractory period. Nonetheless, phenomenological models often need to model refractoriness and this is commonly done by fixing the threshold at infinity during an absolute refractory period of fixed duration and then allowing it to relax towards its resting value during the relative refractory period. The absolute refractory period is considered to be stimulus-independent and so during this period all stimulation is ignored. During the following refractory period, threshold recovery is modelled by one of the many functions introduced in Section 3. These refractory functions, however, have been derived from physiological experiments using only a two-pulse paradigm and therefore accurately describe nerve behaviour only in the absence of further stimulation. We have shown that even for stimulation as simple as two pulses in rapid succession, such models of refractoriness may fail to capture a fibre's recovery correctly. If the stimulation under consideration is more complex than widely-spaced pairs of pulses (e.g., the stimuli in Fig. 8) then the stimulus-dependent nature of the relative refractory period must be considered to obtain an accurate phenomenological model.

Acknowledgements

This work was funded in part by the MRC (grant G0001114) and the EPSRC (grant GR/35650/01).

Appendix A. The Frankenhaeuser-Huxley nerve model

The relative membrane potential, V, for the Frankenhaeuser-Huxley nerve model (Frankenhaeuser and Huxley, 1964) is given by:

$$\frac{\mathrm{d}V}{\mathrm{d}t} = \frac{I_{\mathrm{C}}}{C_{\mathrm{m}}} \tag{A.1}$$

where I_{c} is the capacity current and C_{m} is the membrane capacitance. I_{c} is given by the difference between the stimulating current, I_{in}, and four ion channel currents:

$$I_{\mathrm{C}} = I_{\mathrm{in}} - \left(I_{\mathrm{Na}} + I_{\mathrm{K}} + I_{\mathrm{p}} + I_{\mathrm{L}} \right) \tag{A.2}$$

Here, I_{Na} is the current due to sodium ion channels, I_{K} is the current due to potassium channels, I_{p} represents a non-specific current and I_{L} the leak current. These currents are given by:

$$I_{\mathrm{Na}} = \bar{P}_{\mathrm{Na}} h m^2 \frac{EF^2}{RT} \frac{[\mathrm{Na}]_{\mathrm{o}} - [\mathrm{Na}]_{\mathrm{i}} \exp\left(EF/RT\right)}{1 - \exp\left(EF/RT\right)}, \tag{A.3}$$

$$I_{\mathrm{K}} = P'_{\mathrm{K}} n^2 \frac{EF^2}{RT} \frac{[\mathrm{K}]_{\mathrm{o}} - [\mathrm{K}]_{\mathrm{i}} \exp\left(EF/RT\right)}{1 - \exp\left(EF/RT\right)}, \tag{A.4}$$

$$I_{\mathrm{p}} = \bar{P}_{\mathrm{p}} p^2 \frac{EF^2}{RT} \frac{[\mathrm{Na}]_{\mathrm{o}} - [\mathrm{Na}]_{\mathrm{i}} \exp\left(EF/RT\right)}{1 - \exp\left(EF/RT\right)} \tag{A.5}$$

and

$$I_{\mathrm{L}} = g_{\mathrm{L}} \left(V - V_{\mathrm{L}} \right), \tag{A.6}$$

with $V = E - E_r$. $[Na]_i$ and $[Na]_o$ are the sodium concentrations inside and outside the nerve, respectively, and $[K]_i$ and $[K]_o$ are the inside and outside potassium concentrations. E is the absolute membrane potential, E_r is the membrane resting potential, F is Faraday's constant, R is the gas constant, and T is the absolute temperature. $\overline{P}_{Na}$ and P'_K are the sodium and potassium permeability constants, respectively, $\overline{P}_p$ is the non-specific permeability constant and g_L is the leak conductance.

The gating variables h, m, n and p are variables for the state of various ion channels: m and h are the variables for sodium channel activation and inactivation, respectively, n is the variable for potassium channel activation and p is the variable for non-specific channel activation. They are determined by the following one-dimensional ordinary differential equations:

$$\frac{dh}{dt} = \alpha_h(1-h) - \beta_h h, \tag{A.7}$$

$$\frac{dm}{dt} = \alpha_m(1-m) - \beta_m m, \tag{A.8}$$

$$\frac{dn}{dt} = \alpha_n(1-n) - \beta_n n \tag{A.9}$$

and

$$\frac{dp}{dt} = \alpha_p(1-p) - \beta_p p, \tag{A.10}$$

where the α and β terms (with various subscripts) are functions of the relative membrane potential, V.

References

Abbott, L., Kepler, T., 1990. Model Neurons: From Hodgkin-Huxley to Hopfield. In: Garrido, L., (Ed.), Statistical Mechanics of Neural Networks, Vol. 368. Springer-Verlag, Berlin, pp. 5-18.

Adrian, E., Lucas, K., 1912. On the summation of propagated disturbances in nerve and muscle. Journal of Physiology 44, 68-124.

Adrian, E. D., 1914. The temperature coefficient of the refractory period in nerve. Journal of Physiology 48, 453-464.

Amberson, W. R., 1930. The effect of temperature upon the absolute refractory period in nerve. Journal of Physiology 69, 60-66.

Borst, M., Knoblauch, A., Palm, G., 2004. Modelling the auditory system: preprocessing and associative memories using spiking neurons. Neurocomputing 58-60, 1013-1018.

Bruce, I. C., White, M. W., Irlicht, L. S., O'Leary, S. J., Dynes, S., Javel, E., Clark, G. M., 1999. A stochastic model of the electrically stimulated auditory nerve: Single-pulse response. IEEE Transactions on Biomedical Engineering 46, 617-629.

Bugmann, G., 1997. Biologically plausible neural computation. BioSystems 40, 11-19.

Buller, A., Nicholls, J., Ström, 1953. Spontaneous fluctuations of excitability in the muscle spindle of the frog. Journal of Physiology 122, 409-418.

Chapeau-Blondeau, F., Godivier, X., Chambet, N., 1996. Stochastic resonance in a neuron model that transmits spike trains. Physical Review E 53, 1273-1275.

Erlanger, J., Gasser, H. S., Bishop, G. H., 1927. The absolute refractory phase of the alpha, beta and gamma fibers in the sciatic nerve of the frog. American Journal of Physiology 81, 473-474.

Fitzhugh, R. A., 1961. Impulses and physiological states in theoretical models of nerve membrane. Biophysical Journal 1, 445-.

Forbes, A., Ray, L. H., Griffith, F. R., Jr., 1923. The nature of the delay in the response to the second of two stimuli in nerve and in nerve-muscle preparation. American Journal of Physiology 66, 553-617.

Frankenhaeuser, B., Moore, L. E., 1963. The effect of temperature on the sodium and potassium permeability changes in myelinated nerve fibre of Xenopus laevis. Journal of Physiology 169, 431-437.

Frankenhaeuser, B., Huxley, A. F., 1964. The action potential of the myelinated nerve fibre of Xenopus laevis as computed on the basis of voltage clamp data. Journal of Physiology 171, 302-315.

Frijns, J. H. M., ten Kate, J. H., 1994. A model of myelinated nerve fibres for electrical prosthesis design. Medical and Biological Engineering and Computing 32, 391-398.

Gotch, F., 1910. The delay of the electrical response of nerve to a second stimulus. Journal of Physiology 40, 250-274.

Gotch, F., Burch, G. J., 1899. The electrical response of nerve to two stimuli. Journal of Physiology 24, 410-426.

Hodgkin, A. L., Huxley, A. F., 1952. A quantitative description of membrane current and its application to conduction and excitation in nerve. Journal of Physiology 117, 500-544.

Holden, A., 1976. Models of the stochastic activity of neurons. Springer-Verlag, Berlin.

Litvak, L. M., Delgutte, B., Eddington, D. K., 2003. Improved temporal coding of sinusoids in electric stimulation of the auditory nerve using desynchronizing pulse trains.

Journal of the Acoustical Society of America 114, 2079-2908.
Miller, C. A., Abbas, P. J., Brown, C. J., 2000. An improved method of reducing stimulus artefact in the electrically evoked whole nerve potential. Ear and Hearing 21, 280-290.
Miller, C. A., Abbas, P. J., Robinson, B. K., 2001. Response properties of the refractory auditory nerve fiber. Journal of the Association for Research in Otolaryngology 2, 216-232.
Morse, R. P., Evans, E. F., 2003. The sciatic nerve of the toad *Xenopus laevis* as a physiological model of the human cochlear nerve. Hearing Research 182, 97-118.
Morse, R. P., Allingham, D. A., Stocks, N. G., 2014. A phenomenological model of myelinated nerve with a dynamic threshold. Journal of Theoretical Biology Submitted for publication.
Nagumo, J., Arimoto, S., Yoshizawa, S., 1962. An active pulse transmission line simulating nerve axon. Proceedings of the Institute of Radio Engineers 50, 2061-2070.
Paintal, A. S., 1966. The influence of diameter of medullated nerve fibres of cat on the rising and falling phases of the spike and its recovery. Journal of Physiology 184, 791-811.
Rattay, F., 1990. Electrical Nerve Stimulation: Theory, Experiments and Applications Springer-Verlag, New York.
Rosenblueth, A., Alanís, J., Mandoki, J., 1949. The functional refractory period of axons. Journal of Cellular and Comparative Physiology 33, 405-439.
Taylor, M. M., Creelman, C. D., 1967. PEST: Efficient estimates on probability functions. Journal of the Acoustical society of America 41, 782-787.
Tuckwell, H. C., 1988. Introduction to theoretical neurobiology. Cambridge University Press, Cambridge.
White, M. W., 1985. Speech and stimulus coding strategies for cochlear implants. In: Schindler, R. A., Merzenich, M. M., Eds.), Cochlear implants. Raven Press, New York, pp. 243-267.
Xu, Y., Collins, L. M., 2004. Predicting the threshold of pulse-train electrical stimuli using a stochastic auditory nerve model: the effect of stimulus noise. IEEE Transactions on Biomedical Engineering 51, 590-603.

Figure legends

Fig. 1. Simulated membrane voltage for the Frankenhaeuser-Huxley model in response to two 10-μs cathodic pulses, the first 1 dB above the resting threshold and the second 18 dB above the resting threshold; the absolute resting threshold was 60.61 A / m^2. In both plots the first pulse occurred 1 ms after the start of the simulation but in a) the second pulse was after the absolute refractory period (3 ms after the first pulse) and in b) the second pulse was within the absolute refractory period (1.25 ms after the first pulse). The solid line shows the membrane voltage and the dashed line shows the timing of a blanking signal that was zero from 25 μs before each stimulus pulse to 150 μs afterwards; the blanking signal had a value of unity outside these periods but for illustration is arbitrarily shown here with an amplitude of 100 mV. The non-regenerative response to the second pulse in b) was less than 40 mV after the blanking period.

Fig. 2. Threshold recovery of the Frankenhaeuser-Huxley model following an action potential, measured using a two-pulse paradigm. The simulated thresholds to the second (probe) pulse, relative to the resting threshold, for each interpulse interval are shown by the crosses. The solid line shows the least-squares fit of a two time-constant refractory function (Equation 1) and the dashed line shows the fit of a single time-constant refractory function (Equation 2).

Fig. 3. Example of the three-pulse paradigm used to study the effect of stimulation during the refractory period. The first pulse was a conditioning pulse 1 dB above the resting threshold and with a 10-μs duration. The second pulse was an intermediate pulse, in this example -18 dB below the resting threshold for a 10-μs pulse and 1 ms long, applied immediately following a conditioning pulse. The third pulse was a probe pulse (10-μs duration), which in this example was 6 dB above the resting threshold with an onset 3 ms after the conditioning pulse. Cathodic (excitatory stimulation) is shown by positive values of the current density.

Fig. 4. Threshold recovery of the Frankenhaeuser-Huxley (FH) model following an action potential, measured using a three-pulse paradigm for various amplitudes of a 1000-μs intermediate pulse. The simulated thresholds to the 10-μs probe pulse (the third pulse) against conditioner-probe interval are shown by the symbols for three levels of the intermediate pulse (solid circles: intermediate pulse -30 dB; open circles: intermediate pulse -18 dB; solid triangles: -6 dB). The stimulus levels in dB are relative to the resting threshold of a 10-μs pulse. The dashed lines shows the least-squares fit of a two time-constant refractory function (Equation 1) for each set of recovery data.

Fig. 5. Effect of the amplitude and duration of the intermediate pulse on the refractory parameters. The effects are shown for: (a) the longer refractory time-constant, τ_1; (b) the shorter refractory time-constant, τ_2; (c) the refractory weighting parameter, *k*.; (d) the absolute refractory period, τ_{abs}. The key for the different amplitudes of the intermediate pulse relative to the resting threshold of a 10-μs pulse are given in panel (a).

Fig. 6. Effect of the amplitude of a 2000-μs intermediate pulse on the phase space of the activation and inactivation parameters of the Frankenhaeuser-Huxley model following a 10-μs conditioning pulse 1 dB above threshold. The key for the different amplitudes of the intermediate pulse relative to the resting threshold of a 10-μs pulse are given in panel (a). (a) Phase space for the sodium activation variable, *m*, against the sodium inactivation variable, *h*. (b) Phase space for the sodium activation variable, *m*, against the potassium activation variable, *n*.

Fig. 7. Effect of the amplitude of a 2000-μs intermediate pulse on the time course of the activation and inactivation parameters of the Frankenhaeuser-Huxley model following a 10-μs conditioning pulse 1 dB above threshold. The key for the different amplitudes of the intermediate pulse relative to the resting threshold of a 10-μs pulse are given in panel (a). (a) Sodium activation variable, *m*. (b) Sodium inactivation variable, *h*. (c) Potassium activation variable, *n*. (d) Non-specific activation

variable, *p*.

Fig. 8. Effect of sinusoidal stimulation during the absolute refractory period on the threshold of the Frankenhaeuser-Huxley model. (a) One period of a 100-Hz sinewave that was preceded and followed by a 1-ms gap. The amplitude of the sinewave was 12 dB relative to the threshold for a continuous 100-Hz sinewave (3.52 A / m^2). (b) Stimulus as in (a) except for a gap between 2.0 and 3.5 ms. (c) Sinewave segment that complemented the gap in the stimulus in (c), i.e. (b) and (c) sum to give the stimulus in (a). (d), (e), and (f) show the simulated membrane voltages in response to the stimuli shown in (a), (b), and (c), respectively. The dashed lines in (d), (e), and (f) show the 40-mV threshold used for spike discrimination (see main text).

Figure 1 (2 columns)

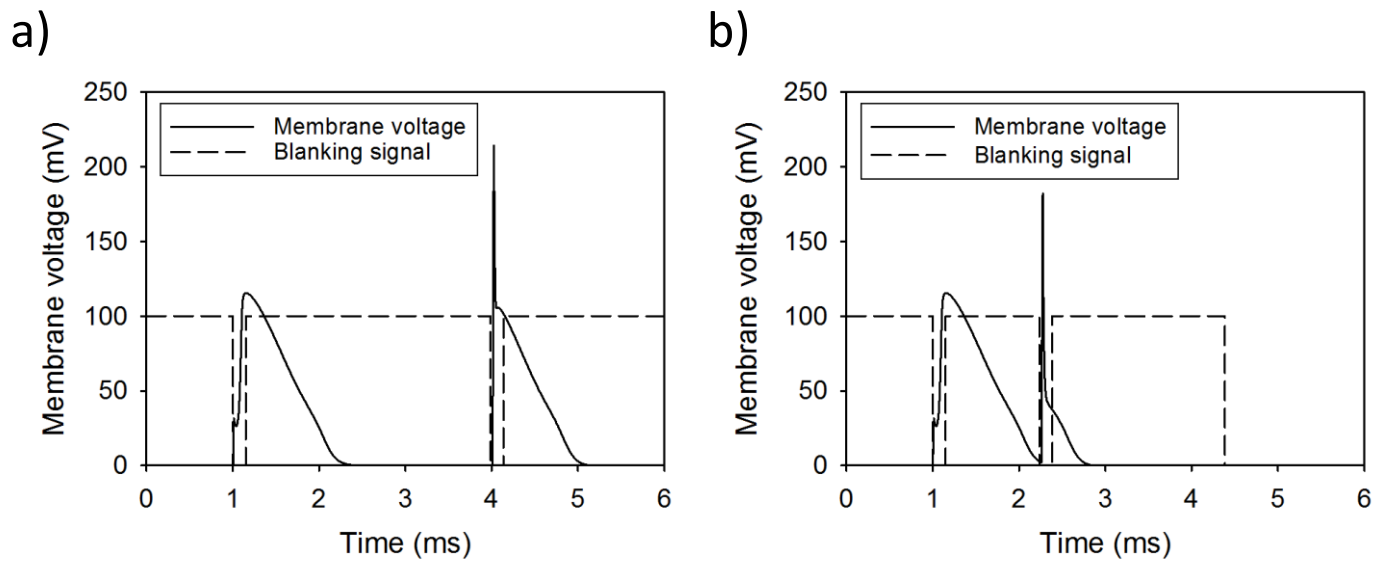

Figure 2 (1 column)

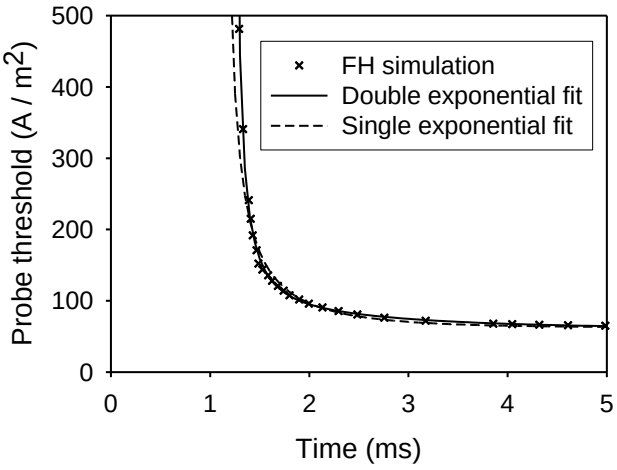

Figure 3

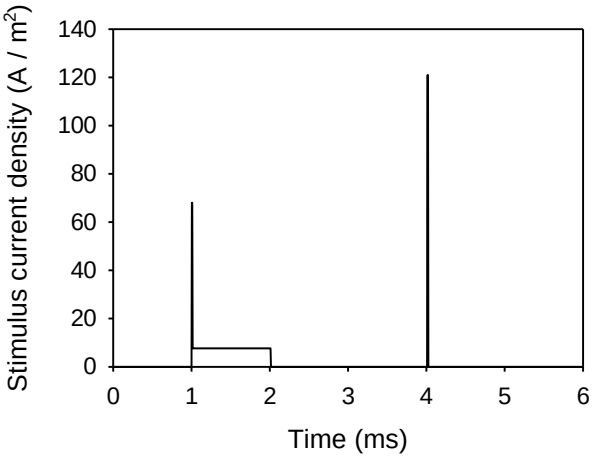
Stimulus current density (A / m2)
140
120
100
80
60
40
20
0
0
1
2
3
4
5
6
Time (ms)

Figure 4 (1 column)

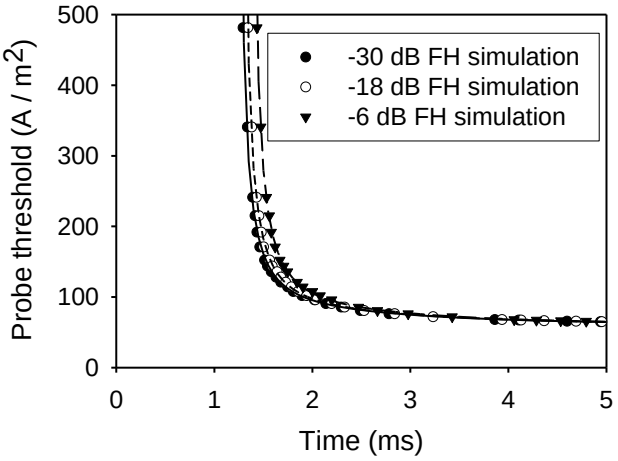

Figure 5 (2 columns)

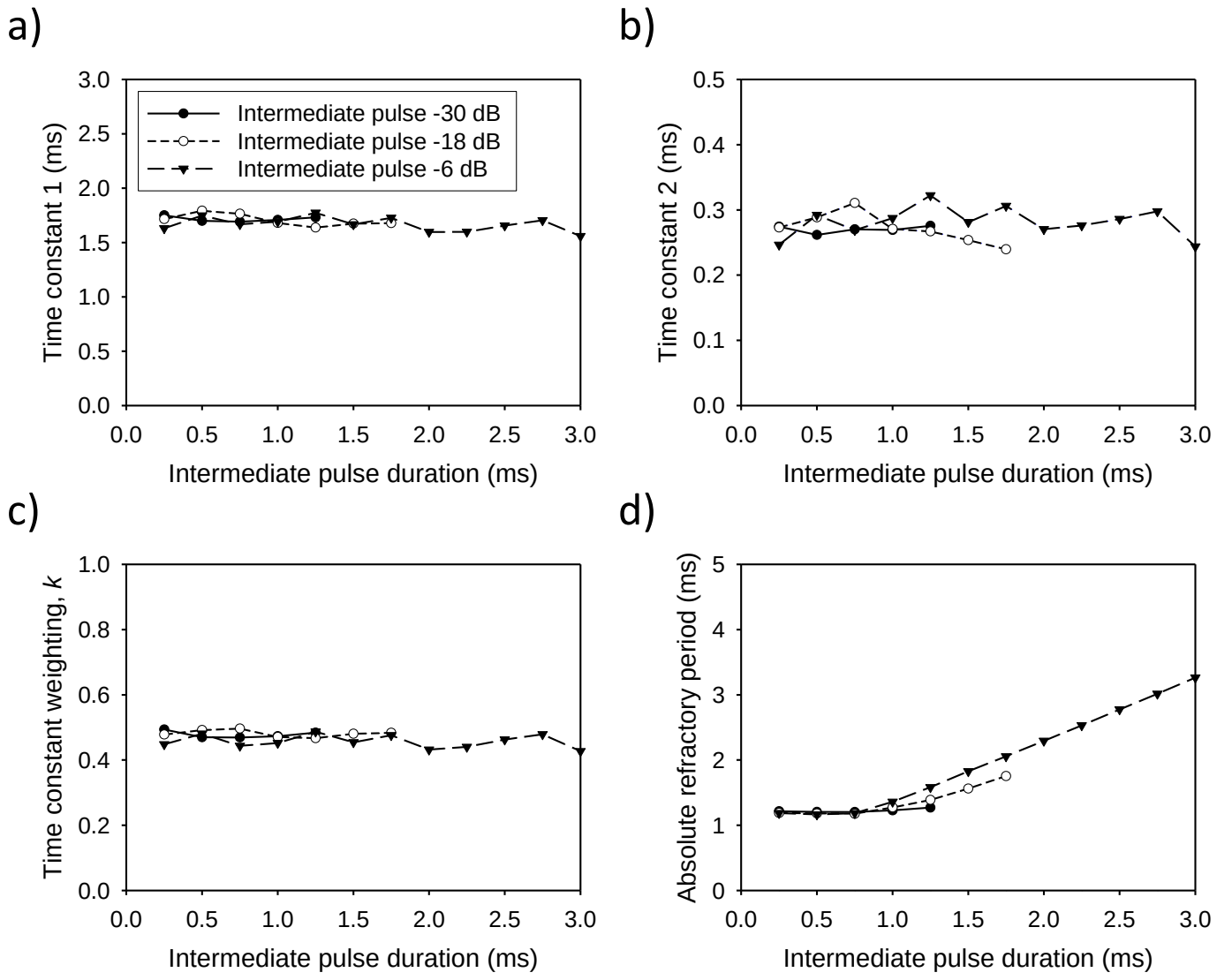

Figure 6 (2 columns)

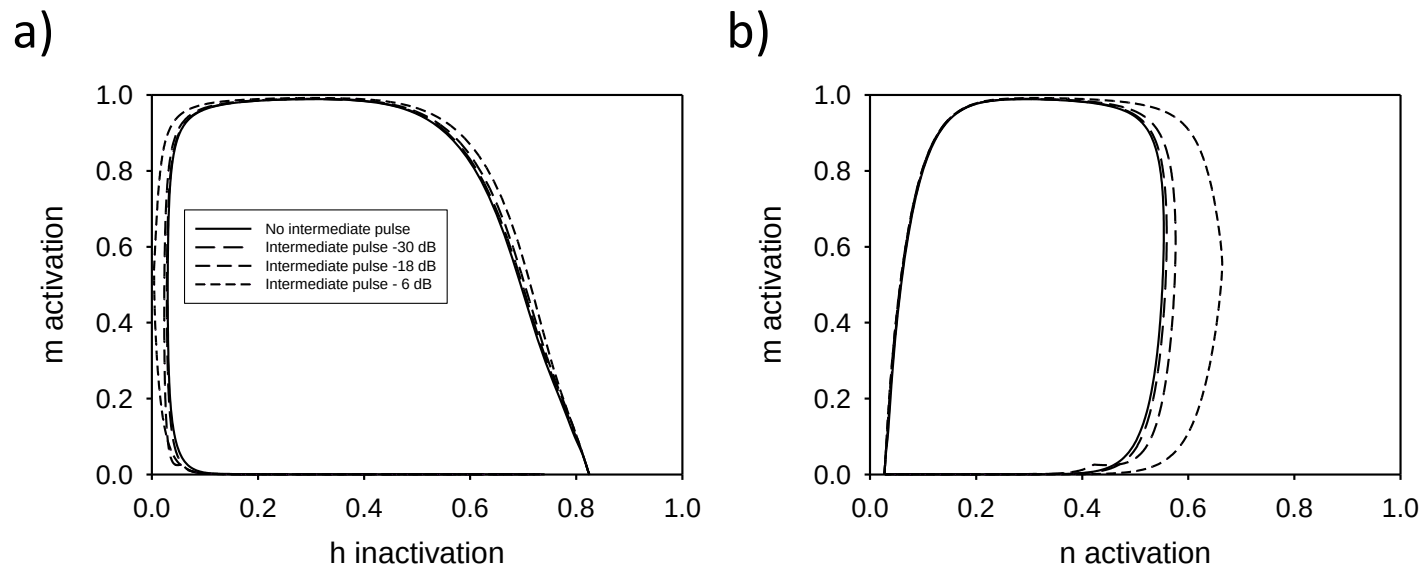

Figure 7 (2 columns)

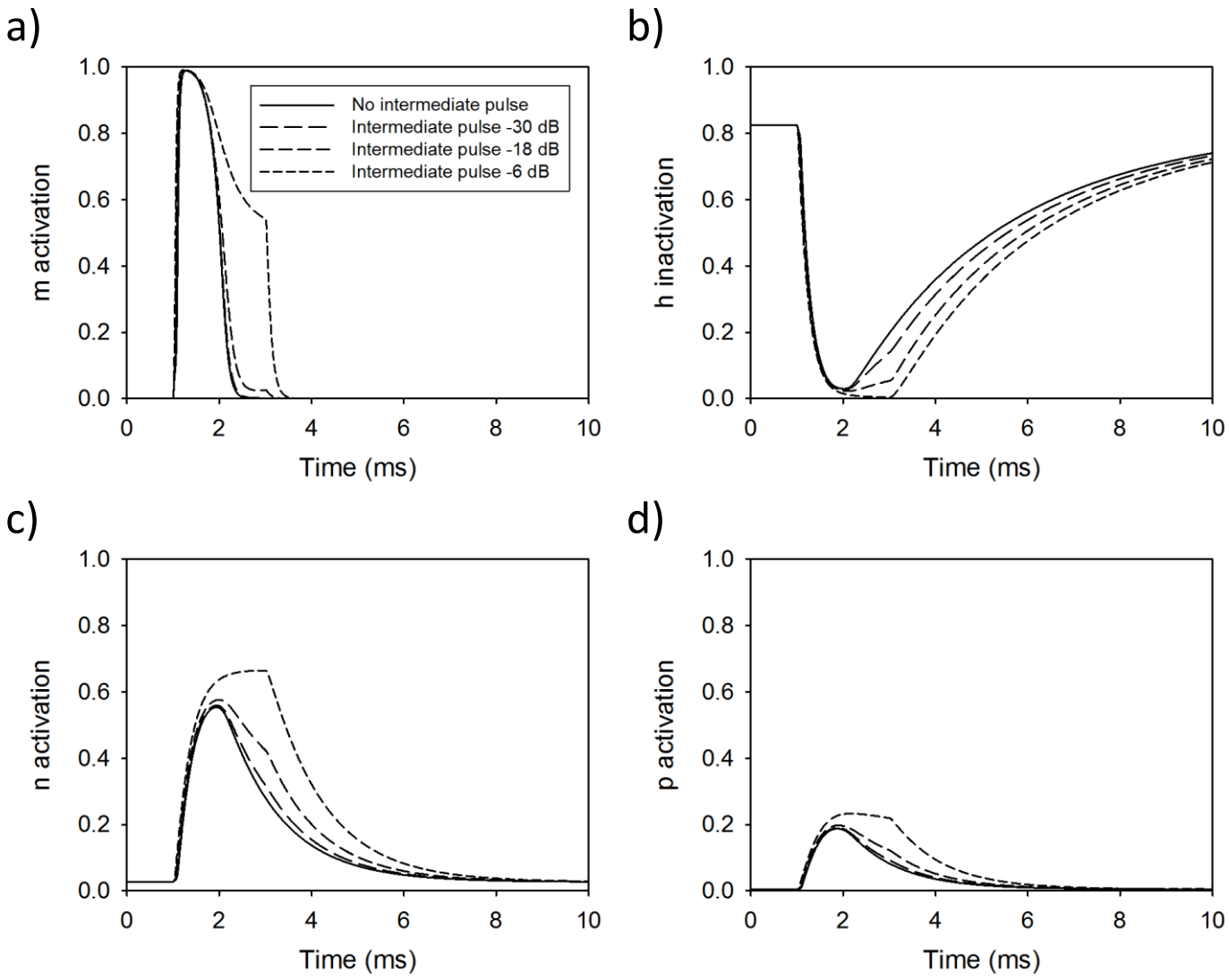

Figure 8 (2 columns)